Journal of Engineering and Development, Vol. 16, No.3, Sep. 2012 ISSN 1813- 7822

Experimental Study on Geogrid-Reinforced Subbase over Soft Subgrade Soil under Repeated Loading

Saad Farhan Ibrahim
Assistant Professor
Assistant Professor; Dept. of HWYS & Transportation- University of Al-Mustansiriya;
Email:drsaadfarhan@gmail.com

Gandhi Ganem Sofia
Assistant Professor
Assistant Professor; Dept. of HWYS & Transportation- University of Al-Mustansiriya;
Email:gandhisofia@yahoo.com

Abbaas Inaayah Kareem
Assistant Lecturer
Graduate Research Assistant; Dept. of HWYS & Transportation- University of Al-Mustansiriya;
Email:kkkabbaas@yahoo.com

Abstract

The present work investigates the behavior of unpaved road overlying soft clay layer reinforced with single layer of geogrid placed at the subgrade/subbase interface. A laboratory model is reinforced with two different types of geogrid and subjected to repeated load using Wheel Tracking Apparatus. Unreinforced and reinforced subbase over soft subgrade were constructed in a large testing box (500mm*500mm*750mm). The test results show that for the same rutting value (75mm); the using of geogrid reinforcement layer produces an increase in number of passes and stress distribution angle and a decrease in displacement on the soft subgrade surface on the reinforced models as the equivalent unreinforced one.

Keywords: *Geogrid Reinforcement; Unpaved road; Soft soil; Rutting.*

دراسة تطبيقية لطبقة ما تحت الاساس مسلحة بمشبك بلاستيكي فوق تربة ضعيفة تحت التحميل المتكرر

الخلاصة

العمل الحالي يتحرى تصرف طريق غير مبلط فوق تربة طينية ضعيفة مسلح بطبقة واحدة من المشبك البلاستيكي موضوعة بين التربة الضعيفة و طبقة السبيس. موديل مختبري سلح بنوعين مختلفين من المشبك البلاستيكي و عرض لحمل متكرر بأستخدام جهاز الـ (Wheel Tracking Apparatus). طبقة سبيس غير مسلحة و أخرى مسلحة فوق تربة ضعيفة تم أنشاؤها في صندوق فحص كبير (500ملم*500ملم*750ملم). نتائج الفحوصات أظهرت بأنه لنفس قيمة التخدد (75ملم)،

أستخدام طبقة تسليح من المشبك البلاستيكي تنتج زيادة في عدد مرات المرور وزاوية نشر الأجهادو تقليل في الازاحة على سطح التربة الضعيفة للنماذج المسلحة أذا ما قورنت بالنماذج غير المسلحة.

Introduction

The concept of adding a reinforcement geosynthetic layer to the subbase/base granular material of unpaved road system has been evaluated by many researchers over the three- four decades. The experimental research takes the form of full scale test, Fannin and Sigurdsson (1996), Hufenus et al. (2005), laboratory plate loading tests conducted in a large test box, Leng (2002), Palmeira and Antunes (2010), Qian and et al. (2010) and laboratory or field tests to evaluate the performance of geosynthetic reinforcement when exposed to the field conditions. Unpaved roads are a two-layer system consisting of a natural subgrade and a subbase course. There are many cases when soil making up the existing subgrade is too weak to support the traffic loads. Conventional measures used to address soft subgrade soils include excavation of the weak soil and replacement with good fill material, using thick pavement section to distribute the vertical load over a large area of the subgrade, chemical stabilization or modification of the subgrade with calcium based materials (i.e., cement, lime, fly ash) which increase strength and improve bearing capacity. Utilizing new technologies to improve pavement performance and increase its service life has recently become an important part of designing and rehabilitating pavement systems. In the past three decades, many different technologies have been introduced as systems that may improve pavement performance and reduce its current premature failures. The use of geosynthetics in the field of pavement design and rehabilitation has increased within the last three decades in the U.S. and abroad. Their use, which began in the early 1970's, has grown phenomenally, (Al-Qadi and Appea, 2003).

This study investigates the improvement in performance of unpaved road-reinforced with single layer of geogrid placed at soft subgrade/subbase interface and subjected to repeated loading. A total of six model tests represent two series are carried out using two thickness of the subbase layer; 10 cm and 12.5 cm respectively: The first series consists of three models with h=10 cm, where h is the thickness of the subbase layer; one of them is unreinforced (named as **Unreinforced-S1**) and the other two models are reinforced with geogrid layer CE163 (named as **GG1**) and CE131 (named as **GG2**) respectively, named as **GG1-S1** and **GG2-S1.** The second series consists of three models with h=12.5 cm; one of them is unreinforced (named as **Unreinforced-S2**) and the other two models are reinforced with geogrid layer CE163 (**GG1**) and CE131 (**GG2**) respectively, named as **GG1-S2** and **GG2-S2**. The laboratory tests were conducted to investigate the influence of geogrid reinforcement layer on the reduction in rut depth and increase the stress distribution angle i.e. reduced the vertical stress at the interface between the subbase and the subgrade as compared with unreinforced section.

Materials Used

Two types of geogrid (named as GG1 and GG2), were used in this experimental study. The dimensional and technical properties of these two types of geogrid are shown in Table 1 and 2 as provided by **Al_latifia Factory for Plastic Mesh**, in accordance with Saudi Arabian Standard Organization (SASO) Procedures. The subbase is brought from Al_Nibaee quarry, north of Baghdad, this type of subbase is commonly used as a layer in flexible pavement construction. Grain size analysis is performed on subbase in accordance with (BS 1377:1975, Test 7 (B)). The grain size distribution curve is shown in Figure (1). The subbase is classified as GP according to the Unified Soil Classification System (USCS). Figure (2) shows the results of modified compaction test for the subbase used; it is apparent that the maximum dry unit is 2.173gr/cm^3 and the optimum moisture content is 7.2%; the tests were carried out according to (BS 1377:1975, Test 13). The other physical and chemical properties of the subbase used are shown in Table (3), the subbase is classified as class (B) according to the State Commission for Roads and Bridges (SCRB, 2003).

Table (1): Technical & Dimensional Properties of GG1 Geogrid. (As Provided by Manufacturer)

Property	Test Method	Unit	Data
Tensile Strength at 2% Strain	ISO 10319	kN/m	4.3
Tensile Strength at 5% Strain	ISO 10319	kN/m	7.7
Peak Tensile Strength	ISO 10319	kN/m	13.5
Yield Point Elongation	ISO 10319	%	20
Aperture		mm	39x39(±2)
Mass Per unit area	ISO 9864	g/m2	770(±40)

Table (2): Technical & Dimensional Properties of GG2 Geogrid. (As Provided by Manufacturer)

Property	Test Method	Unit	Data
Tensile Strength at 2% Strain	ISO 10319	kN/m	2.7
Tensile Strength at 5% Strain	ISO 10319	kN/m	4.9
Peak Tensile Strength	ISO 10319	kN/m	8.5
Yield Point Elongation	ISO 10319	%	20
Aperture		mm	26x26
Mass Per unit area	ISO 9864	g/m2	650

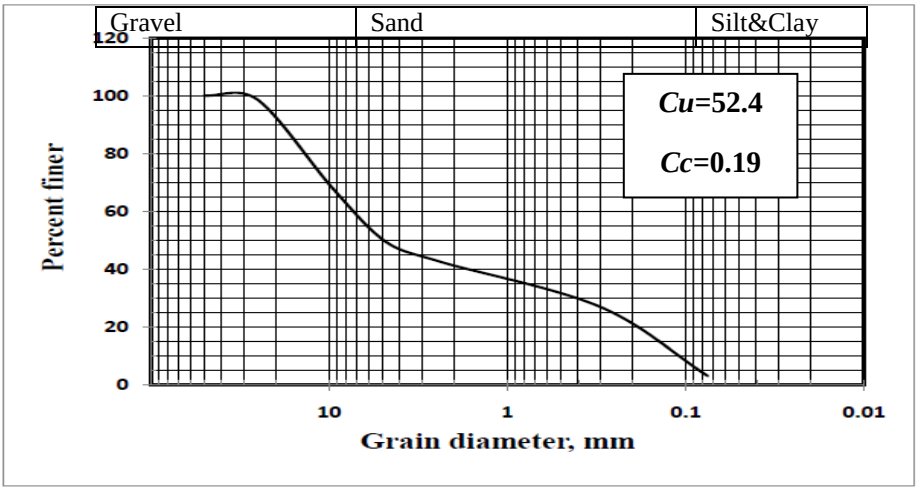

Figure (1): Grain Size Distribution of the Subbase used.

The soft subgrade was white kaolin clay brought from Duitla, west of Baghdad, to prepare the soft subgrade soil in the model. Standard tests are performed to determine the physical properties of the Kaolin, and the results are shown in Table (4).

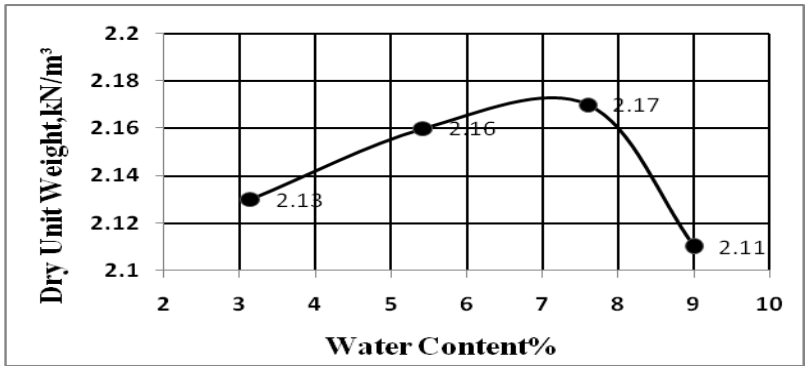

Figure (2): Moisture -Density Relationship for subbase used.

Table (3): Physical and Chemical Properties of the Subbase used.

Index Property	Index Value	Test Method
CBR	44	ASTM D 1883
Liquid Limit%(LL)	NL	AASHTO T 89
Plasticity Index%(PL)	NP	AASHTO T 90
SO3 Content%	0.4	BS 1377 test No. 9
Total Dissolved Salt TDS%	5.33	Earth manual of U.S.
Gypsum Content%	0.86	AASHTO T 112
Organic Matter%	0.05	Test No. 8 of BS 1377

Table (4): Physical Properties of Kaolin.

Physical properties	Index Value	Standards
Specific gravity(G.S)	2.58	ASTM: D -854 -02
Liquid Limit (L.L. %)	57	ASTM: D -4318-00
Plastic Limit (P.L. %)	27	ASTM: D -4318-00
Plasticity Index (PI %)	30	
Soil Symbols(USCS)	CH	

Wheel Tracking Apparatus

This apparatus is used in this study to apply repeated loading to the model of soft soil and a compacted subbase layer in steel container of 750*500*500 mm. Plate No. (1) shows the wheel Tracking Apparatus. New rubber tire is manufactured with 250mm diameter and 100mm width and the contact area between the surface of the subbase layer and the tire is computed, as shown in Plate No. (2).

Steel Container

Two steel containers of 750*500*500 mm are made to host the soft soil, subbase and geogrid (in case of the reinforced model). One of them is used to prepare test sample, while the other is used to prepare a second soft soil for the next test. Each steel box is made of five separate parts, so it can be assembled and dissembled. The internal dimensions of the steel container are 750 mm length, 500 mm width and 500 mm depth. The base of the box is perforated in (22-Twenty Two) holes (12 mm diameter) in order to facilitate the dissipation of the pore water during preparation of the bed of the soft soil. Plate No. (3) shows the steel container used.

Plate No. (1): Wheel Tracking Apparatus.

Plate No. (2): Contact Area between Tire and Subbase.

Plate No. (3): Steel Container used.

Model Preparation

The soft soil is prepared by mixing a total of 120kg of kaolin with water by hands at moisture content equal to 37%, Plate No. (4). It is then placed in five layers inside a steel container of 750*500*500 mm, each layer is of about 50 mm thickness which are filled carefully and pressed lightly by a wooden tamper of size 75mm*75mm in order to remove entrapped air. Then, the surface of the top layer is scarped and leveled to be flat enough, as shown in Plate No. (5) and covered with polythene sheet to prevent any loss of moisture. A wooden board of length 740 mm and width of 490 mm is placed on the surface of bed soil. Finally, a weight of 375 kg, Plate No. (6), equivalent to a pressure of 10kPa is applied and left for four days, which gives clay with an undrained shear strength (Cu) of about 15kpa, the undrained shear strength (Cu) of the subgrade is verified by vane shear tests.

Plate No. (4): Mixing of Kaolin.

Plate No. (5): Leveling of the Top Layer.

Plate No. (6): Loading of the Soft Soil.

The construction of the subbase layer was started after four days from the preparation of the soft soil. A predetermined weight of subbase is mixed with water by hands at

moisture content of 7.2%, this weight is sufficient to create a layer of thickness of about (1/5 h, where h= subbase layer thickness). A total of five layers are compacted gently by a wooden tamper of size 75*75 mm, the top layer is leveled using a piece of plywood and finally the small vibratory compactor, with a 450 mm*500 mm tamping plate is used for vibratory compaction. The compaction commences in one side and proceeds to the other side of the steel container. This process is repeated until the desired thickness is achieved; the target dry unit weight is 20kN/m³ at moisture content of 7.2%. This represents a compaction to 95% of the maximum dry density from modified compaction test. The Sand Cone Apparatus was used to check the dry unit of the subbase layer, Plate No. (7).

Plate No. (7): Checking the Unit Weight of

Model Setup

After the preparation of the bed of soft soil, the geogrid layer is placed on the surface of the subgrade soft soil (in case of the reinforced model) and folded in 90̊ against the long side of the steel container, Plates No. (8) and (9), to obtain necessary anchorage and slight pre-tensioning, as well as to prevent shifting of the geogrids out of position, *Tang et al,* (2008).Then, the construction of the subbase layer begins and when this process is complete, the steel container is handled with crane of 5ton capacity and fixed in position. The wheel is placed on the surface of the subbase in such condition that the center of the wheel coincides with the center of the subbase surface. The wheel is then brought in contact with top surface of the subbase, Plate No. (10).

Repeated Loading Test

A total load of 1.74 kN is applied which produces a contact stress of 550 kPa; this represents 100% of the contact stress of the standard axle load (W18). All tests are

applied at speed of 0.85 m/s and the repetition of the load continues until 75 mm rut develops. For all model tests, the failure is defined as the number of load repetitions required to develop rutting equal to 75 mm, Rut depth is defined as the vertical distance between the lowest point in the rut and a line extending between the high points of the subbase surfaces on either side of the rut. Figure (3) shows the intensity of the contact stress above the centerline of the steel container, when the wheel is above the centerline of the steel container, the intensity of the contact stress is equal to 550 kPa and when the wheel is at a distance 190 mm from the centerline the intensity of contact stress is equal to zero, Huang (2004).

Plate No. (8): Folding GG1 Geogrid in 90° against the Long Side of Steel Container.

Plate No. (9): Folding GG2 Geogrid in 90° against the Long Side of Steel Container.

Plate No. (10): Coinciding Wheel with the Center of the Subbase Surface.

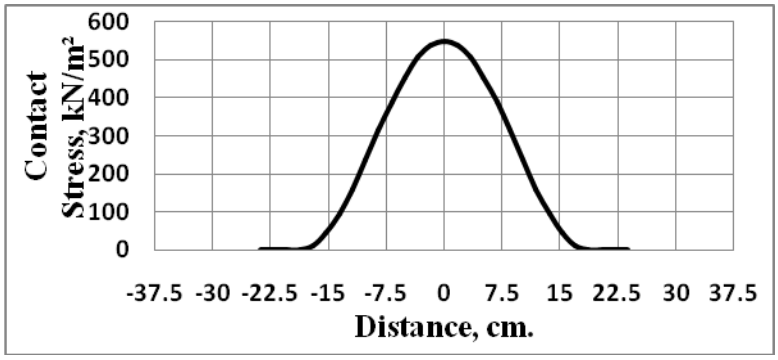

Figure (3): The Intensity of Contact Stress at the Centerline of the Steel Container.

Results and Discussions

Surface Profiles Test Results

The surface profiles for models with h= 10cm (Unreinforced-S1, GG1-S1 and GG2-S1), are shown in Figures (4) to (6) respectively, Figures (7) to (9) respectively show the surface profile for models with h=12.5cm (Unreinforced-S2, GG1-S2 and GG2-S2). The overall results show that the rutting at the center line of wheel paths and the heave outer of wheel paths are accumulated with the number of passes; the rutting and heave increase quickly at the initial passes and the increasing rate decreases with the increase in the number of wheel passes. Maximum heave is observed with unreinforced models; the heave decreases with models reinforced with GG1 geogrid layer and further decrease with models reinforced with GG2 geogrid layer. This is an indication of the effectiveness of GG2 geogrid in restricting the particles of the subbase from the horizontal movement and allowing the wheel to compact subbase layer during the testing process. The GG1 is less effective in this function; this may be attributed to the large aperture size of the GG1 geogrid.

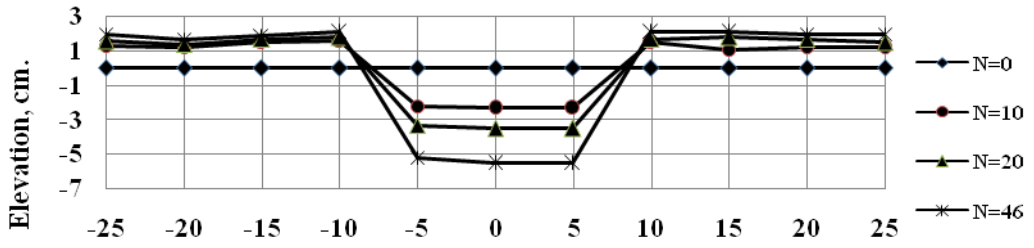

Fig 4: Surface Profile for Unreinforced-S1 Model.

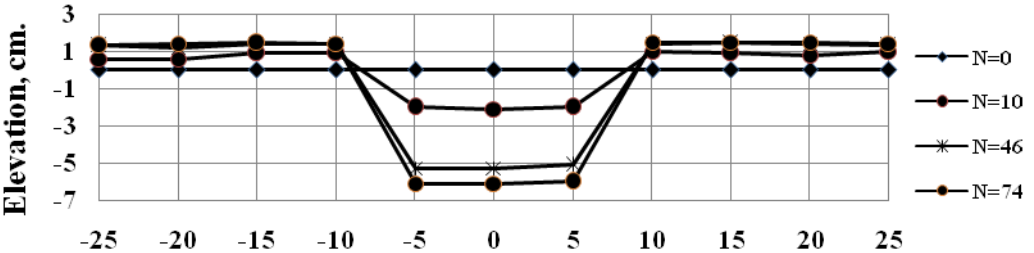

Fig 5: Surface Profile for GG1-S1 Model.

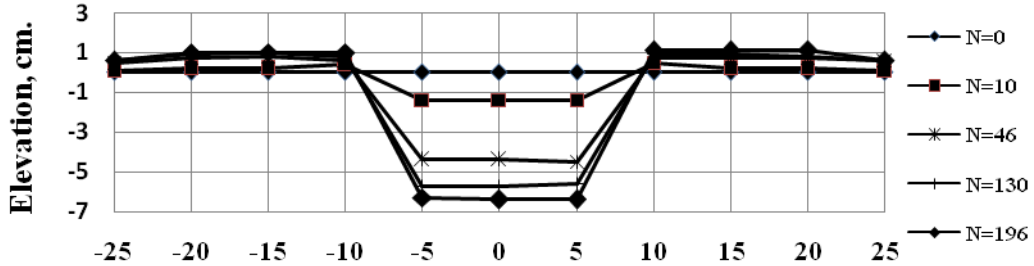

Fig 6: Surface Profile for GG2-S1 Model.

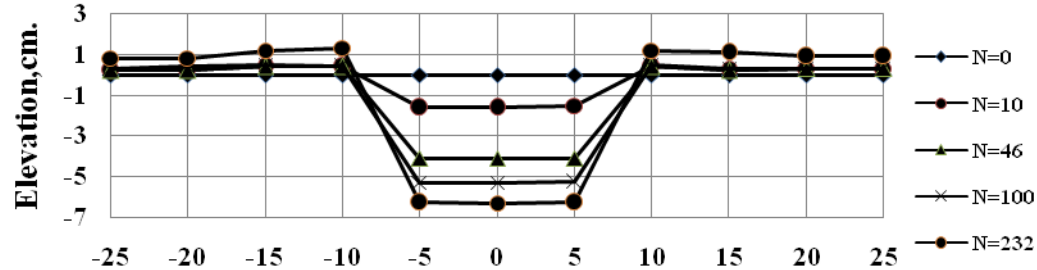

Fig.7: Surface Profile for Unreinforcedd-S2 Model.

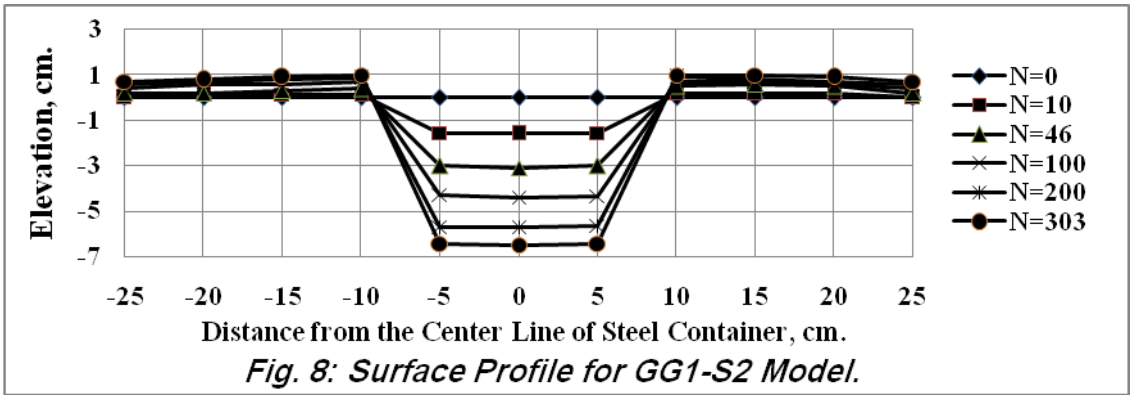

Fig. 8: Surface Profile for GG1-S2 Model.

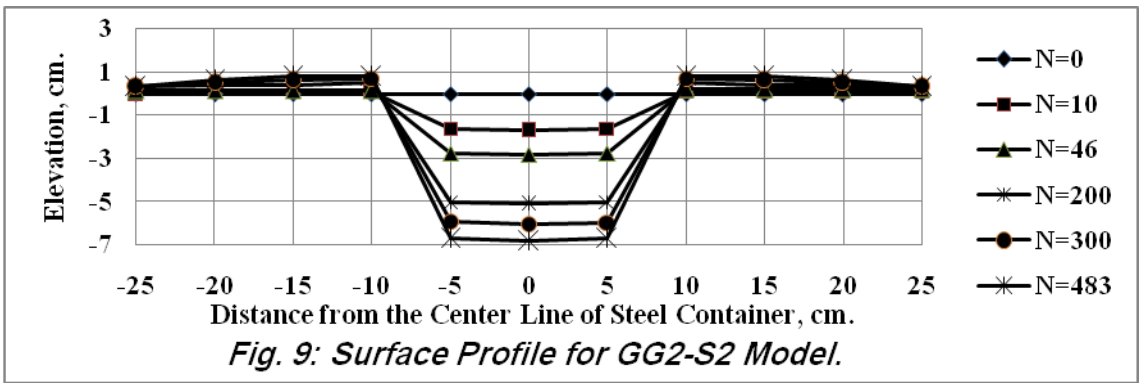

Fig. 9: Surface Profile for GG2-S2 Model.

The test results reveal that:

- For the same model type with different subbase thickness, i.e. **Unreinforced-S1** and **Unreinforced-S2**, the Unreinforced-S2 model needs more wheel passes to reach the same rutting value. Figure (10) shows the increase the number of passes due to increase thickness of the subbase layer.
- For the same model type, the models with 12.5cm subbase thickness have rut cross sectional area smaller than models with 10cm subbase thickness
- Table (5) shows the percent increase in number of passes to reach permanent deformation (rut depth) equal to (75mm) for each of the two models with the same type due to the increase in the subbase thickness from 10cm to 12.5cm. The highest percent increase in number of passes is observed with unreinforced models, where the unreinforced-S2 model has five times the number of passes of Unreinforced-S1 model. This increase in number of passes decreases to become four times the number of passes for model reinforced with GG1 geogrid and further decreases to become two times and a half the number of passes for model reinforced with GG2 geogrid. It seems that the benefit of inclusion a geogrid layer at the subgrade/subbase interface decreases as the thickness of the subbase layer is increased.

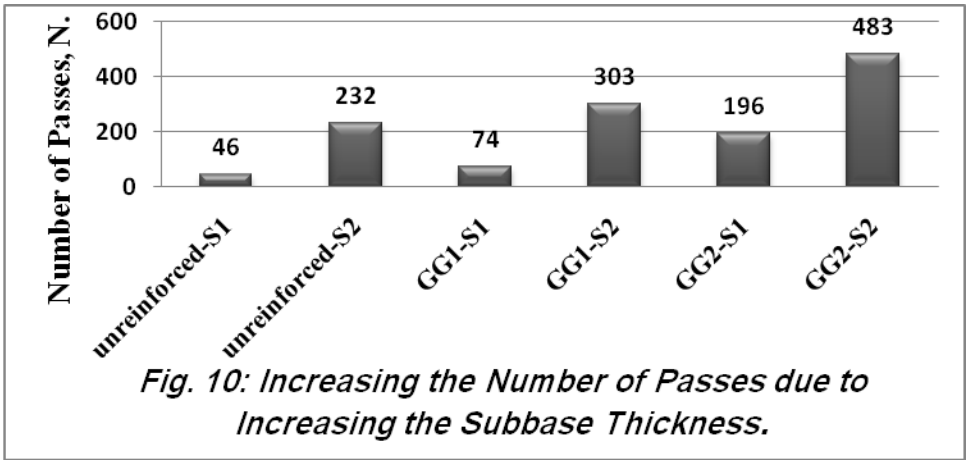

Fig. 10: Increasing the Number of Passes due to Increasing the Subbase Thickness.

Table (5): Percent Increase in Number of Passes due to Increase the Subbase Thickness.

Test	Unreinforced	GG1	GG2
Number of Passes for Models in Series No.1. (S1)	46	74	196
Number of Passes for Models in Series No.2. (S2)	232	303	483
Increase in Number of Passes (%).	503%	409%	246%

Displacement of the Subgrade Surface Test Results

Plates (11) to (13) and Figures (11) to (13) show the subgrade profile at the end of testing process for models in series No.1; Unreinforced-S1, GG1-S1 and GG2-S1 respectively, and Plates (14) to (16) and Figures (14) to (16) show the subgrade profile at the end of testing process for models in series No.2; Unreinforced-S2, GG1-S2 and GG2-S2 models respectively. The test results reveal that the displacement on the subgrade surface is variable, with maximum value below the centerline of wheel paths. The maximum displacement value occurs with unreinforced models and decreases with reinforced models. The test results show that the displacement value decreases with inclusion geogrid layer at the subgrade/subbase interface and the reinforcement layer leads to more flatten deformed shape on the subgrade surface. The flatten deformed shape of the subgrade is related to more relatively uniform distributed stress on the subgrade surface and this is one of the main functions of the geogrid reinforcement which distributes load over a large area. The GG1geogrid is less effective in decreasing the displacement value than the GG2 geogrid; this may be attributed to the large aperture size of GG1 geogrid (39*39 mm).

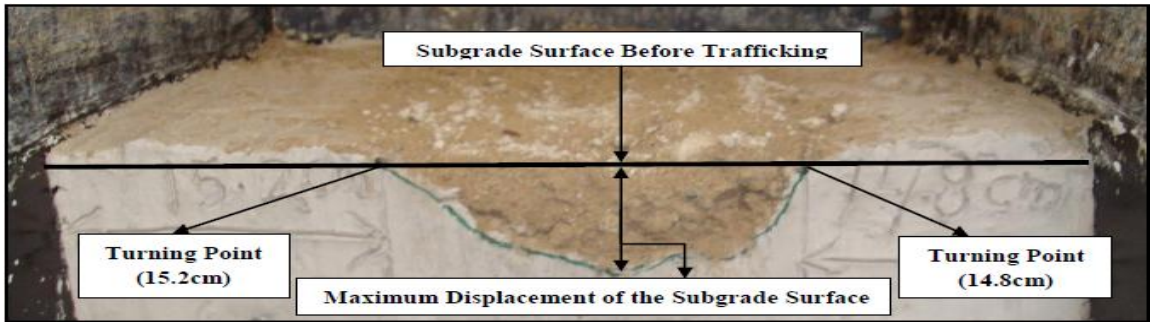

Plate No.(11): Subgrade Profile for Unreinforced-S1Model.

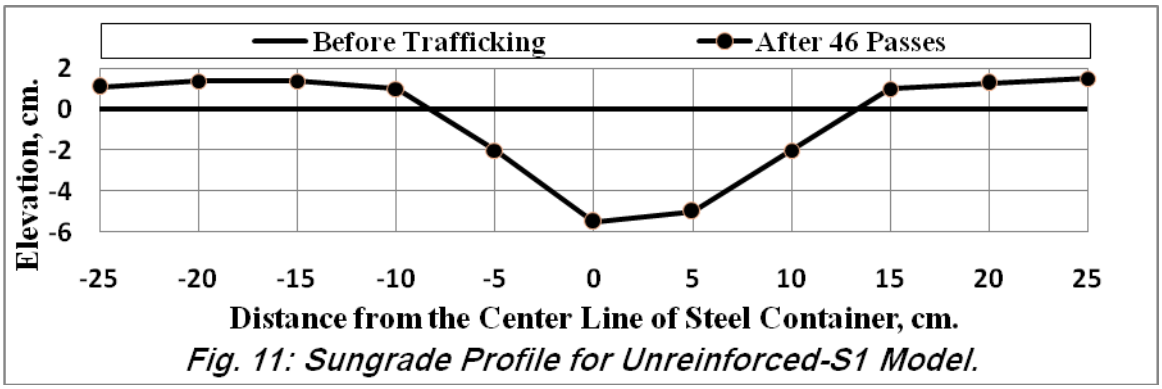

Fig. 11: Sungrade Profile for Unreinforced-S1 Model.

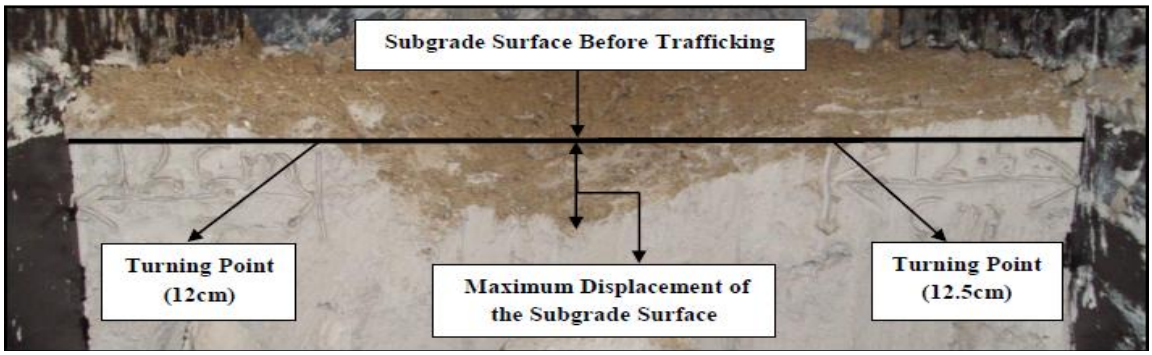

Plate No.(12): Subgrade Profile for GG1-S1 Model.

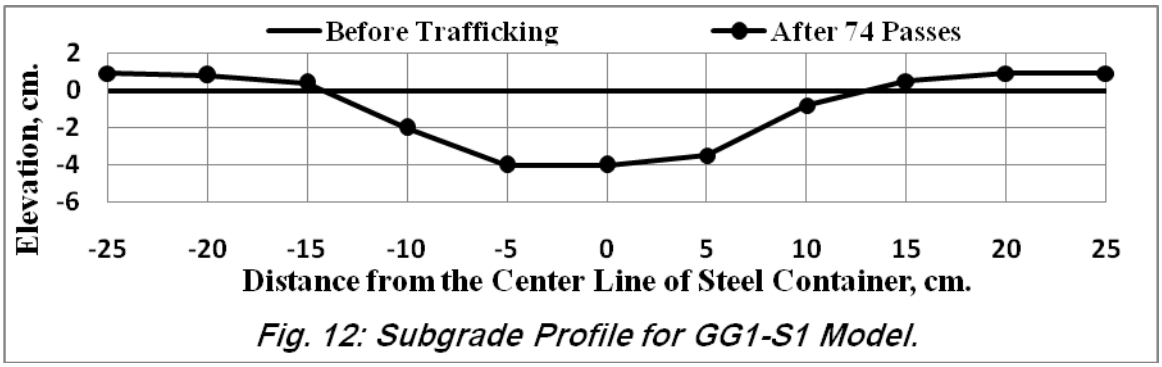

Fig. 12: Subgrade Profile for GG1-S1 Model.

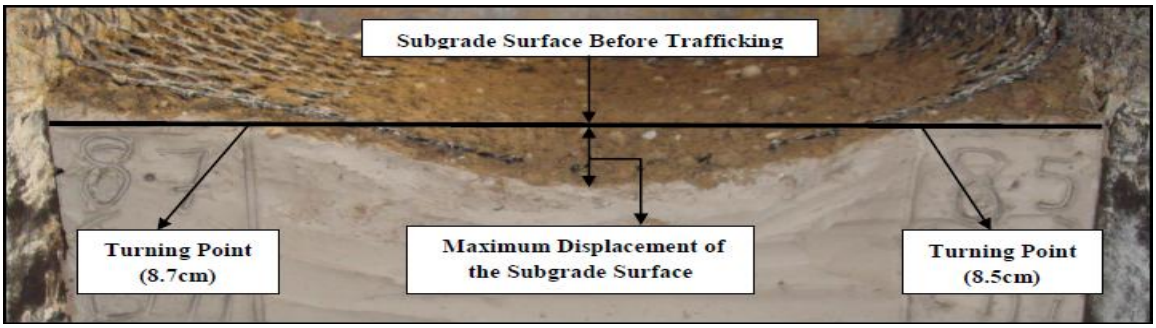

Plate No. (13): Subgrade Profile for GG2-S1 Model.

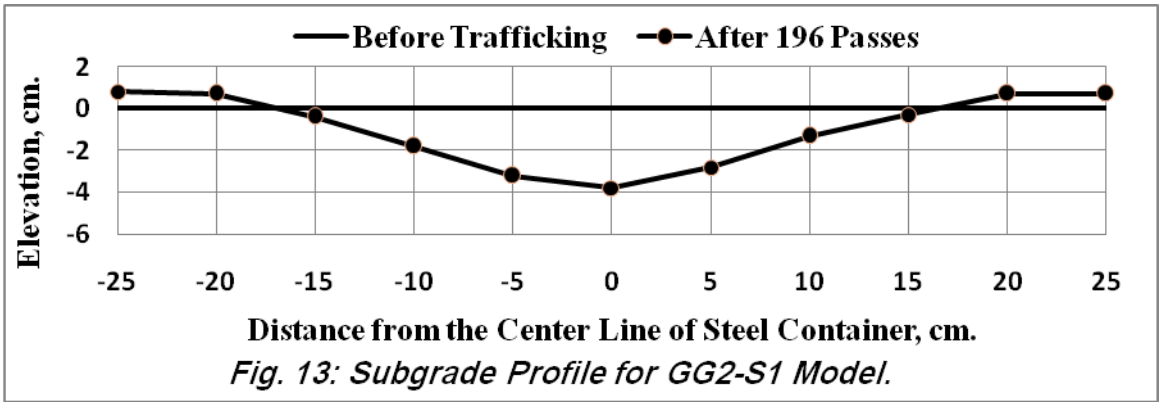

Fig. 13: Subgrade Profile for GG2-S1 Model.

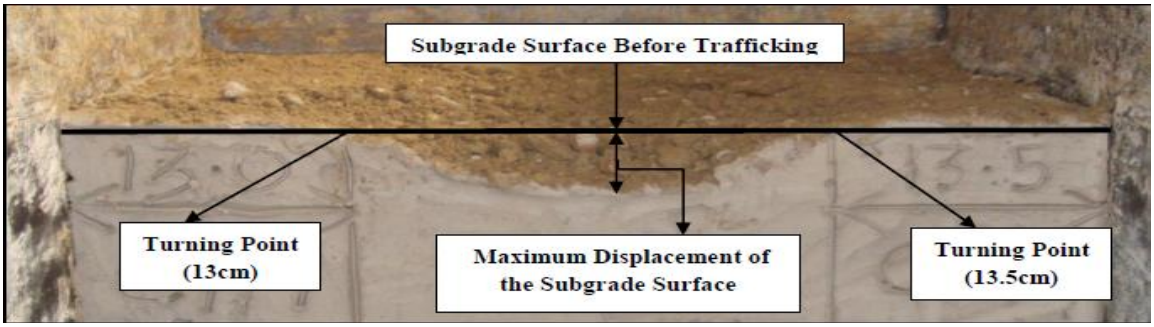

Plate No. (14): Subgrade Profile for Unreinforced-S2 Model.

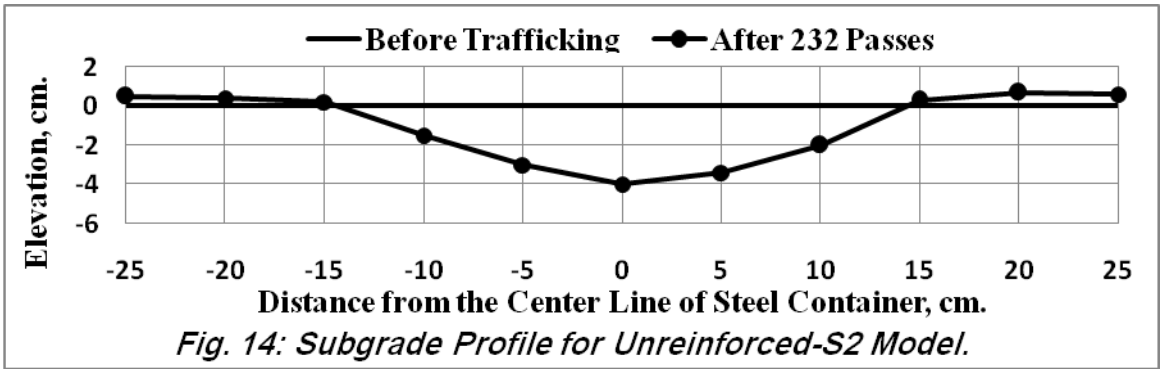

Fig. 14: Subgrade Profile for Unreinforced-S2 Model.

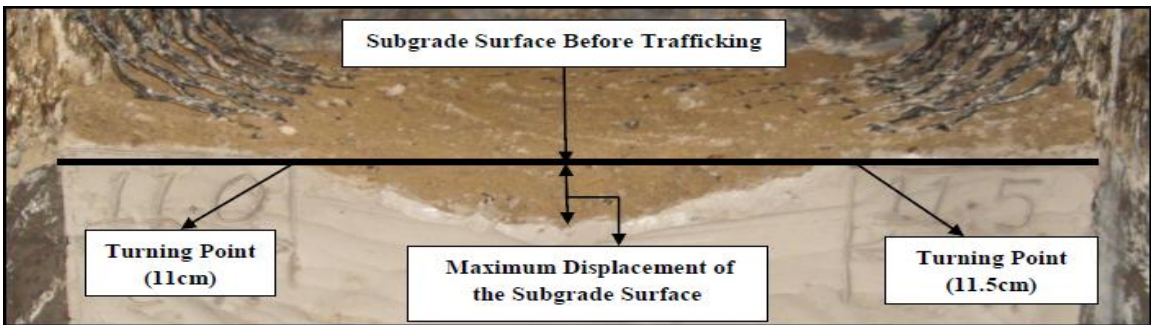

Plate No. (15): Subgrade Profile for GG1-S2 Model.

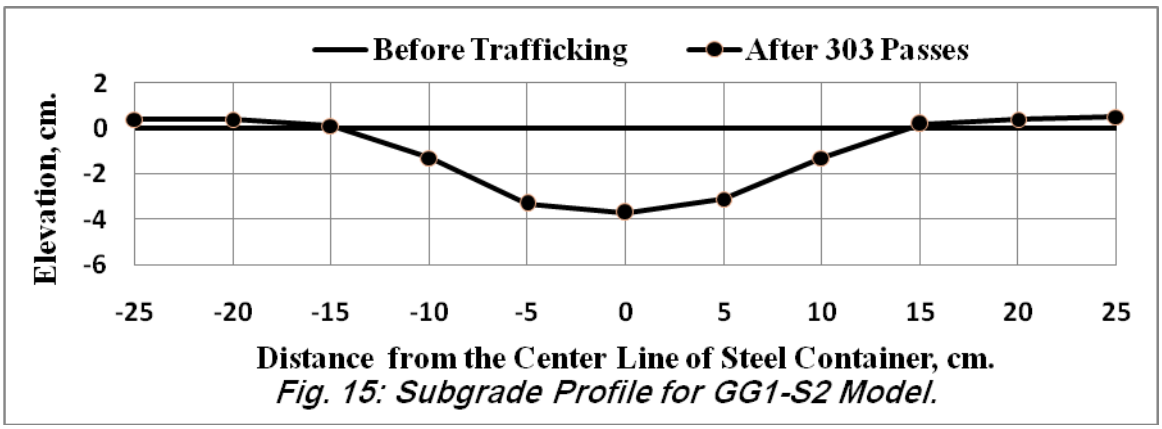

Fig. 15: Subgrade Profile for GG1-S2 Model.

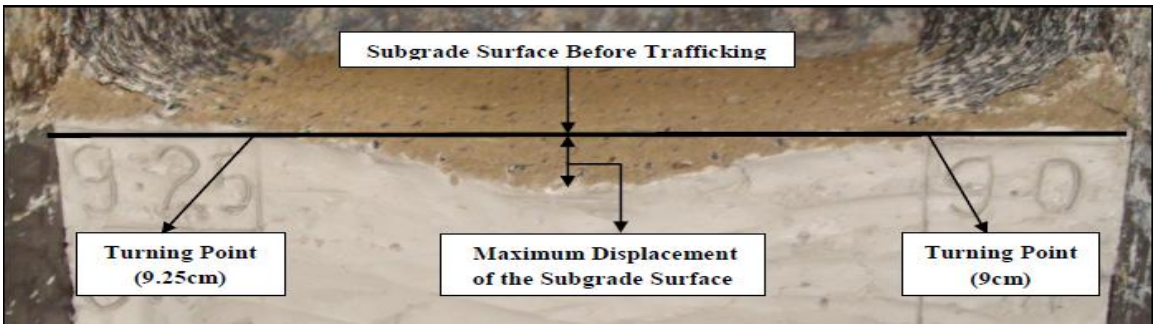

Plate No. (16): Subgrade Profile for GG2-S2 Model.

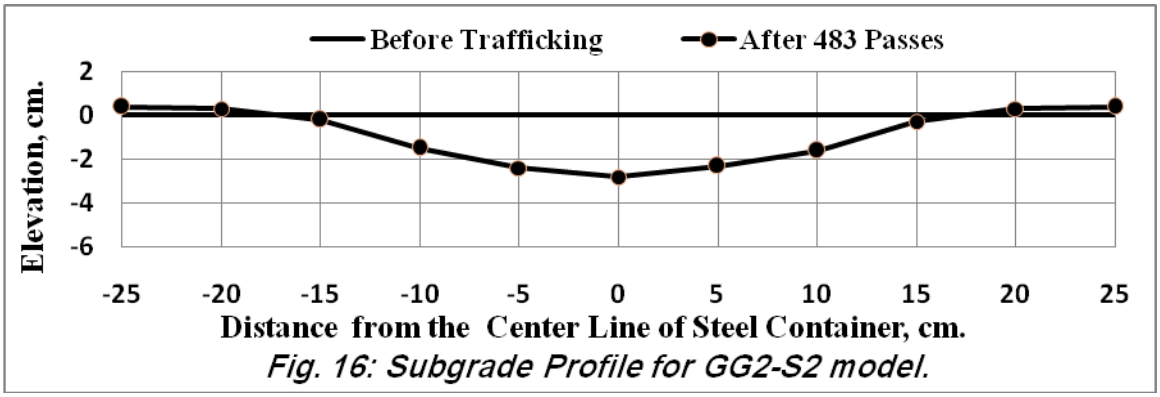

Fig. 16: Subgrade Profile for GG2-S2 model.

The overall results show:

- For the same model type, the models in series No.2 have less magnitude of the displacement than the models in series No.1, for example; the displacement for Unreinforced-S1 model is (55mm) while the displacement for Unreinforced-S2 model is (40mm). Figure (17) shows the reduction in maximum displacement on the subgrade surface at the end of the testing process for the 6 model tests.
- Table (6) shows the percent reduction in displacement due to increase in the subbase thickness, which is equal to %27 for unreinforced models and %7.5, %26 for models reinforced with GG1 and GG2 geogrid layer respectively. It seems that the benefit of placing a geogrid layer at the subgrade/subbase interface decreases as the thickness of subbase is increased.

Table (6): Percent Reduction in Maximum Displacement.

Test	Unreinforced	GG1	GG2
Displacement of Subgrade Surface for Models in Series No.1, cm.	5.5	4	3.8
Displacement of Subgrade Surface for Models in Serise No.2, cm.	4	3.7	2.8
%Reduction	27%	7.5%	26%

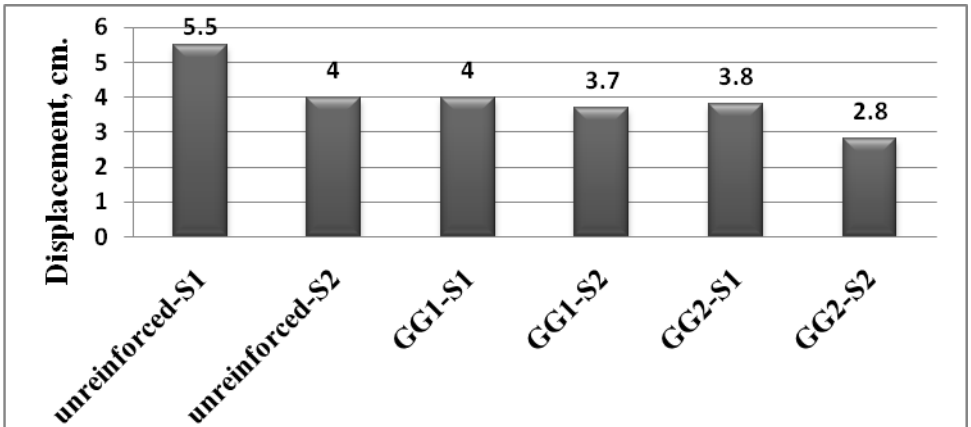

Fig. 17: Reduction in Maximum Displacement due to Increasing the Subbase Thickness.

Turning Point and Stress Distribution Angle Test Results

The turning point for Unreinforced-S1 model lies at a distance of 15cm {(14.8+15.2)/2, Plate No. (11)} from the long side of the steel container. This distance decreases with GG1-S1 model and becomes 12.25cm {(12.5+12)/2, Plate No (12)}, and further decreases with GG2-S1 model and becomes 8.6cm {(8.7+8.5)/2, Plate No. (13)}, for models with subbase thickness equal to 12.5cm the turning point for Unreinforced-S2 model lies at distance of 13.25cm {(13+13.5)/2, Plate No. (14)} from the long side of the steel container. This distance decreases with GG1-S2 model and becomes 11.25cm {(11+11.5)/2, Plate No. (15)} and further decreases with GG2-S2 model and becomes 9.1cm {(9.25+9)/2, Plate No. (16)}. with these locations for the turning points, the stress distribution angle can be computed for each model; For Unreinforced-S1 model: Tan (α) =[{width of the steel container-(2*distance from the long side of the steel container)-width of the wheel}/2]/thickness of the subbase layer=[{50-(2*15)-10}/2]/10= 5/10 therefore α= 26.5˚, for GG1-S1 and GG2-S1 models (α) is equal to 37.7˚ and 48.7˚ respectively, for models in series No.2 (α) equal to 28.36˚, 35˚ and 41˚ for Unreinforced-S2, GG1-S2 and GG2-S2 models respectively.

The overall result shows:

- The geogrid reinforcement layer placed at subgrade/subbase interface distributed wheel load over large area, and the GG2 geogrid is more effective in this function than GG1 geogrid. This may be attributing to good interlocking between the subbase particles and GG2 aperture size.
- Increasing the subbase thickness produces an increase in stress distribution angle from α=26.5˚ for Unreinforced-S1 model to α=28.36˚ for Unreinforced-S2 model, while this

increase in thickness produces a decrease in stress distribution angle from α=37.7˚ and α=48.7˚ for GG1-S1 and GG2-S1 models to α=35˚ and α=41˚ for GG1-S2 and GG2-S2 models. It is obvious that the geogrid reinforcement effectiveness decreases with the increase in the thickness of subbase layer. Figure (18) shows the stress distribution angle for all model tests.

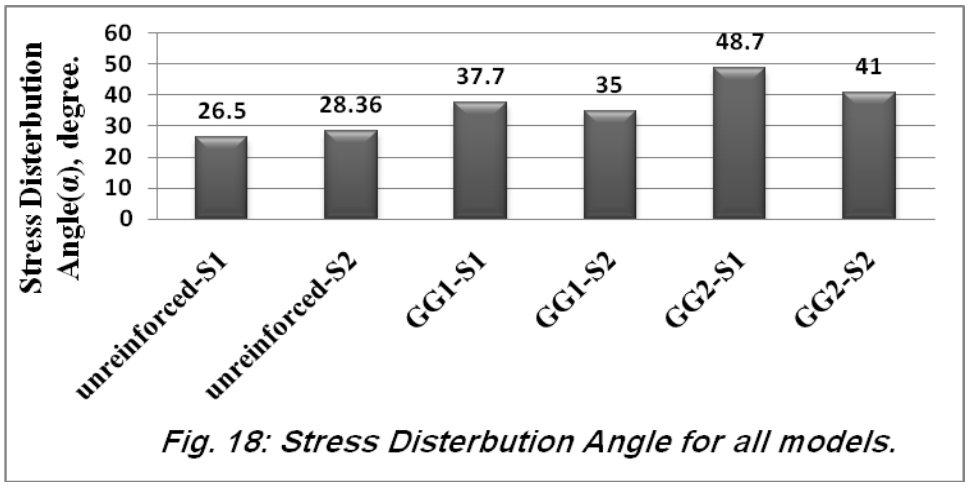

Fig. 18: Stress Disterbution Angle for all models.

Relationship Between Rut Depth (r) and Number of Passes (N) and Subbase Thickness (h)

Figure (19) shows the relationship between rut depth(r), number of passes (N) and thickness of the subbase layer (h) for models in series No.1. The response of the Unreinforced-S1 model shows a rapid permanent deformation development (rutting) during the initial number of passes and fails at 46 passes (reach rut depth equal to 75mm)., The GG2-S1 model shows relatively considerable difference in response and exhibits a stable response to wheel passes while the GG1-S1 model is less stable in response to wheel passes. The models reinforced with GG1 and GG2 geogrid layer fail at 74 and 196 passes respectively. This represents a value of ***Traffic Benefit Ratio*** {***TBR***, *defined as the ratio of the number of passes for the reinforced model to that for the unreinforced model at the rut depth of 75mm*} of 1.6 and 4.26 for GG1-S1 and GG2-S2 models respectively. Figure (20) shows the relationship between rut depth(r), number of passes (N) and thickness of the subbase layer (h) for models in series No.2, the Unreinforced-S2 model shows relatively a stable response to the wheel passes and fails at 232 passes. The reinforced models, GG1-S2 and GG2-S2 respectively, exhibit a stable

response to the wheel passes and fail at 303 and 483 passes respectively. This represents a value of TBR of 1.3 and 2.

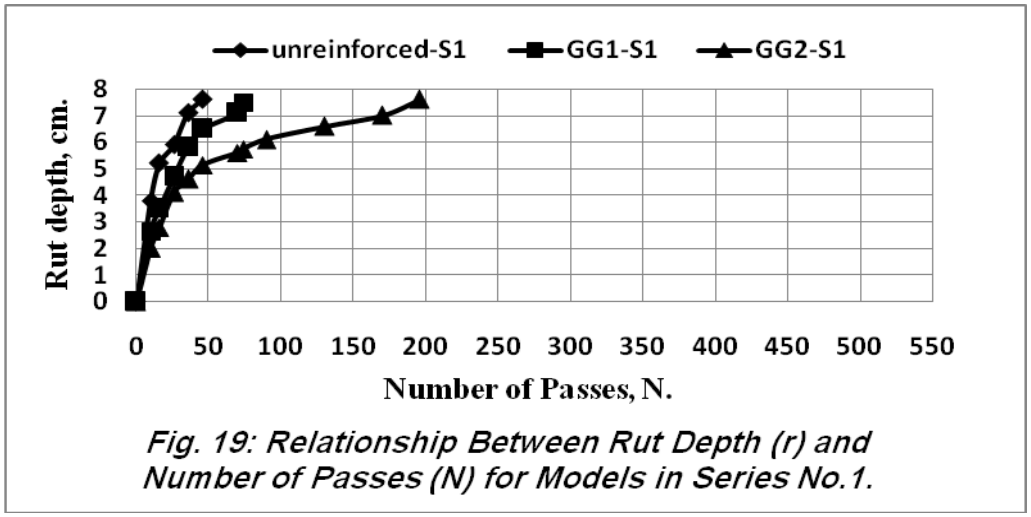

Fig. 19: Relationship Between Rut Depth (r) and Number of Passes (N) for Models in Series No.1.

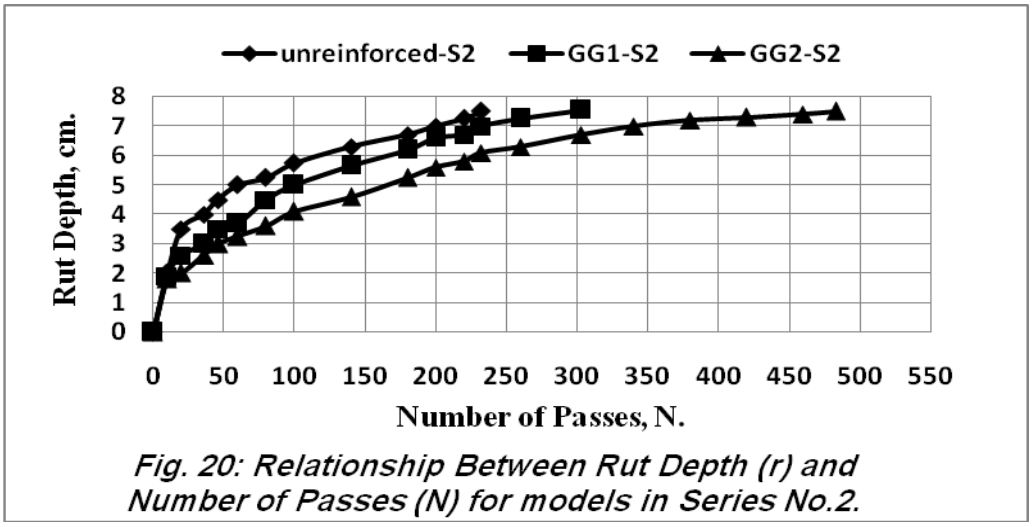

Fig. 20: Relationship Between Rut Depth (r) and Number of Passes (N) for models in Series No.2.

The overall results show:

- The inspection of the curves shows an improvement in the reinforced models over the equivalent unreinforced model and the difference is most significant for the thinner subbase course layers.
- The increase in the subbase thickness leads to a reduction in TBR from 1.6 and 4.26 for GG1-S1 and GG2-S1 models to 1.3 and 2 for GG1-S2 and GG2-S2 models. It is obvious that, increasing the thickness of the subbase produces a reduction in TBR, i.e. less effectiveness to the geogrid reinforcement. Figure (21) shows the reduction in Traffic benefit ratio for reinforced models due to the increase in the subbase thickness.

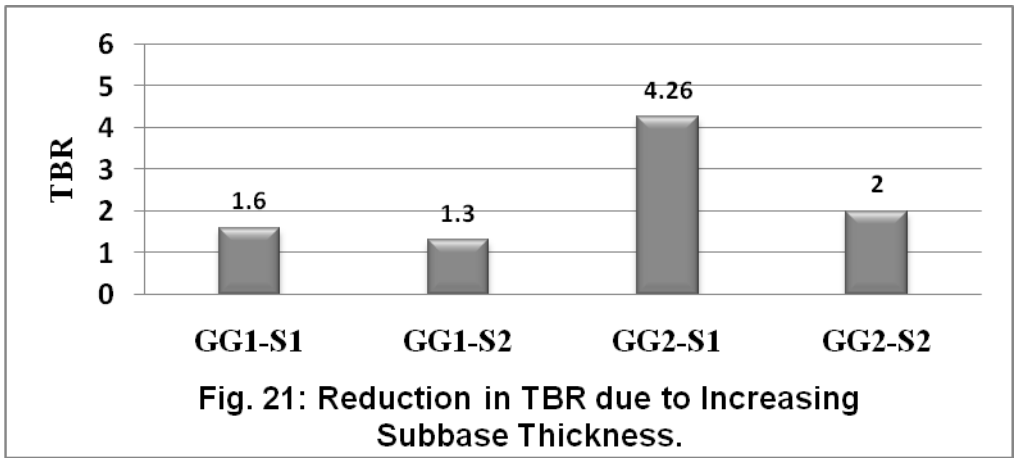

Fig. 21: Reduction in TBR due to Increasing Subbase Thickness.

Conclusions

According to the results and analysis of the six model tests performed, the following conclusions are drawn:

a) The use of geogrid reinforcement produces an increase in the number of passes with reinforced models, and increasing the thickness of subbase leads to increase the number of passes for all model types and the maximum percent increase occurs in unreinforced model.

b) For the same subbase thickness, inclusion of the geogrid layer at the interface between the subbase and subgrade leads to more flatten deformed shape on the subgrade surface, and as a result less displacement value and further increase in subbase thickness leads to further decrease in displacement on the subgrade surface for all models and maximum percent decrease occurs in unreinforced model.

c) The inclusion of geogrid layer at the subgrade/subbase interface distributes the wheel loads over large area, i.e. reduction in the magnitude of the vertical stress at the interface. The results show that increasing subbase thickness leads to increase the (α) values with unreinforced model and decrease the (α) values with reinforced models.

d) Increasing the thickness of the subbase produces a reduction in TBR, i.e. less effectiveness to the geogrid reinforcement and diminishes the difference between the reinforced models and unreinforced models behavior.

Acknowledgments

The authors would like to thank Mr. Jameil Al-razem for providing the geogrid reinforcement.

References

[1]Al-Qadi I.L. and Appea A.K. (2003). "**Eight-Year of Filed Performance of A Secondary Road Incorporating Geosynthetics at the Subgrade-Base Interface**." Transportation Research Board Annual Meeting, pp1-3.

[2]American Society for Testing and Materials, ASTM. (2003). "***soil and Rock (I)***." Vol. 04.08.

[3]Fannin R.J. and Sigurdsson O. (1996). "**Field Observation on Stabilization of Unpaved Roads with Geosynthetics**." ASCE, Journal of Geotechnical Engineering, Vol. 122, No.7, PP. 544-553.

[4]Head K.H., (1984). **"Manual of Soil Laboratory Testing."** Volume 1: Soil Classification and Compaction Tests.

[5]Head K.H., (1984). **"Manual of Soil Laboratory Testing."** Volume 2: Permeability, Shear Strength and Compressibility Tests.

[6]Huang Y.H., (2004). "**Pavement Analysis and Design**." Second Edition, Pearson Education, Inc.

[7]Hufenus R., Rueegger R., Banjac R., Mayor p., Springman S.M. and BrÖnnimann R. (2005)."**Full-scale Field Tests on Geosynthetic Reinforced Unpaved Roads on Soft Subgrade.***"* Geotextiles and Geomembranes 24 (1), pp. 21–37.

[8]Iraqi General Specification for Roads and Bridges, (2003)."**Standard Specification for Roads and Bridges**." The state Commission for Road and Bridges, Revised Edition.

[9]Leng J. (2002). "**Characteristics and Behavior of Geogrid Reinforced Aggregate under Cyclic Load**." Ph.D. thesis, North Carolina state university.

[10]Palmeira E. M. and Antunes L. G. S. (2010). "**Large Scale Tests on Geosynthetic Reinforced Unpaved Roads Subjected to Surface Maintenance**." Geotextiles and Geomembranes 28 (2010), pp. 547-558.

[11]Qian Y., Han J., Pokharel S.K. and Parsons R.L. (2010)."**Experimental Study on Triaxial Geogrid-Reinforced Bases over Weak Subgrade under Cyclic Loading**." ASCE, Conference Proceeding Paper, pp.1208-1215.

[12]Tang X., Chehab G.R. and Palomino A.M. (2008).”**Accelerated Testing of Geogrid-Reinforced Subgrade in Flexible Pavements**.” ASCE, Conference Proceeding Paper, pp. 1049-1055.